NASA/TM—2017-219420

Modeling Xenon Tank Pressurization Using One-Dimensional Thermodynamic and Heat Transfer Equations

Ryan P. Gilligan and Thomas M. Tomsik
Glenn Research Center, Cleveland, Ohio

April 2017

NASA STI Program . . . in Profile

Since its founding, NASA has been dedicated to the advancement of aeronautics and space science. The NASA Scientific and Technical Information (STI) Program plays a key part in helping NASA maintain this important role.

The NASA STI Program operates under the auspices of the Agency Chief Information Officer. It collects, organizes, provides for archiving, and disseminates NASA's STI. The NASA STI Program provides access to the NASA Technical Report Server—Registered (NTRS Reg) and NASA Technical Report Server—Public (NTRS) thus providing one of the largest collections of aeronautical and space science STI in the world. Results are published in both non-NASA channels and by NASA in the NASA STI Report Series, which includes the following report types:

- TECHNICAL PUBLICATION. Reports of completed research or a major significant phase of research that present the results of NASA programs and include extensive data or theoretical analysis. Includes compilations of significant scientific and technical data and information deemed to be of continuing reference value. NASA counter-part of peer-reviewed formal professional papers, but has less stringent limitations on manuscript length and extent of graphic presentations.

- TECHNICAL MEMORANDUM. Scientific and technical findings that are preliminary or of specialized interest, e.g., "quick-release" reports, working papers, and bibliographies that contain minimal annotation. Does not contain extensive analysis.

- CONTRACTOR REPORT. Scientific and technical findings by NASA-sponsored contractors and grantees.

- CONFERENCE PUBLICATION. Collected papers from scientific and technical conferences, symposia, seminars, or other meetings sponsored or co-sponsored by NASA.

- SPECIAL PUBLICATION. Scientific, technical, or historical information from NASA programs, projects, and missions, often concerned with subjects having substantial public interest.

- TECHNICAL TRANSLATION. English-language translations of foreign scientific and technical material pertinent to NASA's mission.

For more information about the NASA STI program, see the following:

- Access the NASA STI program home page at http://www.sti.nasa.gov

- E-mail your question to help@sti.nasa.gov

- Fax your question to the NASA STI Information Desk at 757-864-6500

- Telephone the NASA STI Information Desk at 757-864-9658

- Write to:
  NASA STI Program
  Mail Stop 148
  NASA Langley Research Center
  Hampton, VA 23681-2199

NASA/TM—2017-219420

Modeling Xenon Tank Pressurization Using One-Dimensional Thermodynamic and Heat Transfer Equations

Ryan P. Gilligan and Thomas M. Tomsik
Glenn Research Center, Cleveland, Ohio

National Aeronautics and
Space Administration

Glenn Research Center
Cleveland, Ohio 44135

April 2017

Level of Review: This material has been technically reviewed by technical management.

Available from

NASA STI Program
Mail Stop 148
NASA Langley Research Center
Hampton, VA 23681-2199

National Technical Information Service
5285 Port Royal Road
Springfield, VA 22161
703-605-6000

This report is available in electronic form at http://www.sti.nasa.gov/ and http://ntrs.nasa.gov/

Modeling Xenon Tank Pressurization Using One-Dimensional Thermodynamic and Heat Transfer Equations

Ryan P. Gilligan and Thomas M. Tomsik
National Aeronautics and Space Administration
Glenn Research Center
Cleveland, Ohio 44135

Summary

NASA's Asteroid Redirect Robotic Mission (ARRM) intended to launch a spacecraft that would capture a boulder from a near Earth asteroid, redirect the asteroid, and tow the boulder to a lunar orbit where it could be studied by astronauts. As a first step in understanding what ground support equipment would be required to provide external cooling during the loading of 5000 kg of xenon into the ARRM spacecraft's four aluminum-lined composite overwrapped pressure vessels (COPVs), a modeling analysis was performed using Microsoft Excel. The goals of the analysis were to predict xenon temperature and pressure throughout loading at the launch facility, to estimate the time required to load one tank, and to get an early estimate of what provisions for cooling xenon might be needed while the tanks are being filled. The model uses the governing thermodynamic and heat transfer equations to achieve these goals. Results indicate that a single tank can be loaded in about 15 hr with reasonable external coolant requirements. The model developed in this study was successfully validated against flight and test data. The first dataset is from the Dawn mission, which also utilizes solar electric propulsion (SEP) with xenon propellant, and the second is test data from the rapid loading of a hydrogen cylindrical COPV. The main benefit of this type of model is that the governing physical equations using bulk fluid and solid temperatures can provide a quick and accurate estimate of the state of the propellant throughout loading, which is much cheaper in terms of computational time and licensing costs than a computational fluid dynamics analysis while capturing the majority of the thermodynamics and heat transfer.

Introduction

The Asteroid Redirect Robotic Mission (ARRM) plans to use 5 to 10 t of xenon as a propellant for its spacecraft's solar electric propulsion (SEP) system. One challenge associated with this large propellant load is transferring the xenon into the spacecraft's flight propellant tanks in a timely manner while the spacecraft is on the launch pad. The time required to fill the flight tanks for NASA's Dawn spacecraft, which also used xenon propellant, was discovered to be directly proportional to the xenon's heat of compression generated during loading in addition to external cooling heat transfer rates (Ref. 1). Figure 1 (Ref. 2) displays the cylindrical xenon tanks for the Block 1A TT7 Eight Tank Configuration. The xenon load per tank is 2000 kg, so the eight tanks in Block 1A represent a previously considered 16-t mission scenario (Ref. 3). After ARRM's Mission Concept Review (MCR), the decision was made to downsize the xenon tanks to hold a 1250-kg xenon load. This paper describes a Microsoft Excel model of xenon propellant transfer into the smaller, post-MCR flight tanks. Symbols used in this paper are defined in the Appendix.

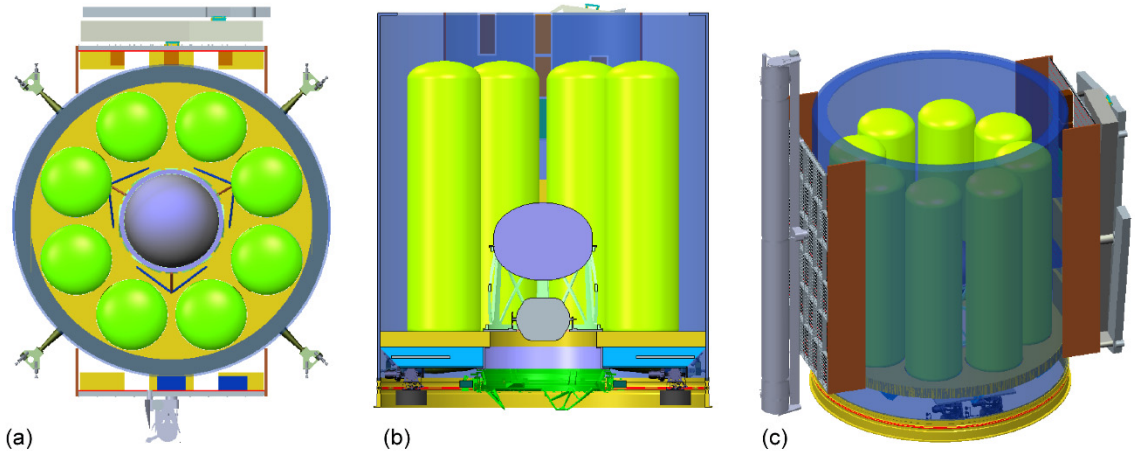

Figure 1.—Asteroid Redirect Robotic Mission (ARRM) Solar Electric Propulsion (SEP) Block 1A TT7 Eight Tank Configuration (Ref. 2).

Model Development

The model considers the loading of a single composite overwrapped pressure vessel (COPV). The xenon inside the flight tank is assumed to be initially at 14.7 psia and 20 °C, which corresponds to a 7 kg initial propellant load. The inlet gas temperature is assumed to be controlled at a constant 20 °C; this would be achieved via a heat exchanger within the supply line. For ground processing at the launch facility, the xenon must be maintained in a supercritical state and its temperature cannot exceed 55 °C during loading in order to avoid exceeding the tank maximum design temperature. The state of the tank at a fully loaded condition is required to be 1750 psia at 40 °C. The constant mass flow rate of xenon is an additional required input.

Figure 2 shows the control volume considered and illustrates the assumed direction of heat transfer. The variables listed in Figure 2 as P, T, and m are the pressure, temperature, and mass of xenon gas inside the COPV, respectively. The constant assumed mass flow rate into the tank is $\dot{m}_{\text{in}}$, and $h_{0\text{in}}$ is the stagnation enthalpy of gas entering the tank. Assuming a uniform COPV wall temperature, T_w, greatly simplifies the analysis, and the ambient temperature T_∞ is also assumed constant. $\dot{Q}_i$ is the heat transfer rate between the gas and the tank wall, $\dot{Q}_\infty$ is the heat transfer rate between the tank wall and the ambient environment, and v_∞ is the velocity of the coolant gas outside the tank.

Performing an energy balance on the inside of the tank and following the convention of Figure 2 yields

$$\frac{d}{dt}(mu) = -\dot{Q}_i + \dot{m}_{\text{in}} h_{0\text{in}} \tag{1}$$

Unless otherwise specified, lack of a subscript implies that the property pertains to the gas within the vessel being charged. Performing an energy balance on the wall of the COPV yields

$$\frac{dU_w}{dt} = (W_c)_w \left(\frac{dT_w}{dt}\right) = \dot{Q}_i - \dot{Q}_\infty \tag{2}$$

where $(W_c)_w$ is the effective heat capacitance of the COPV wall, $\frac{dU_w}{dt}$ is the change in wall internal energy with respect to the change in time, and $\left(\frac{dT_w}{dt}\right)$ is the change in wall temperature with respect to the change in time (Ref. 4). The COPV is assumed to be composed of a 0.03-in.-thick (0.76-mm)

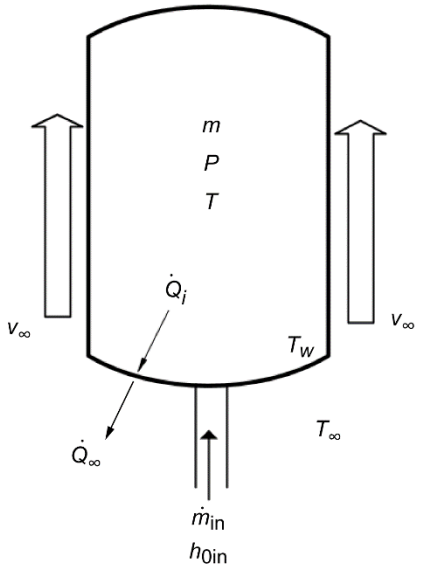

Figure 2.—Control volume used in xenon loading analysis and relevant parameters.

TABLE I.—ASSUMED THERMAL AND MASS PROPERTIES OF COMPOSITE OVERWRAPPED PRESSURE VESSEL (COPV) USED IN ASTEROID REDIRECT ROBOTIC MISSION (ARRM) ANALYSIS

Material	Mass, kg	Specific heat, J/kg-K	Thermal capacitance, J/K
Aluminum liner	13	900	11,700
T1000 fiber	48	754	36,192
Cured epoxy resin	1	2,090	2,090
Total	62	-------	49,982

aluminum liner with a 0.19-in.-thick (4.8-mm) Toray T1000 fiber composite overwrap attached using a 0.007-in. (0.18-mm) epoxy film adhesive. To determine the thermal capacitance of the tank, the mass of each material was multiplied by its respective heat capacity and these were summed to determine the total thermal capacitance. The assumed COPV properties are listed in Table I (Ref. 3).

Equation (3) provides the heat transfer rate between the xenon gas inside the vessel and the vessel wall (Ref. 4).

$$\dot{Q}_i = \left(h_q A_w\right)_i \left(T - T_w\right) \tag{3}$$

In Equation (3), $\left(h_q A_w\right)_i$ is the product of the convection coefficient between the xenon gas and the tank wall and the surface area of the inside of the vessel. Due to a lack of theoretical or empirical correlations for forced convection in the charging of tanks that do not require heavy computational techniques such as computational fluid dynamics (CFD), only free convection was considered for the inside surface. According to research by Lyons, the heat transfer coefficient for the charging of a vessel with gas "can be estimated within one order of magnitude by free convection theories. The heat transfer coefficient thus obtained will be equal to or less than the actual value" (Ref. 5). Ranong studied the rapid loading of hydrogen tanks and determined that the tangential velocity along the inside tank wall was always less than 4 percent of the inlet velocity (Ref. 6). While the ratio of tangential wall velocity to inlet flow velocity will vary based upon the gas species, Ranong's research found that the ratio was independent of the mass flow rate. Assuming that changing from hydrogen to xenon does not have an overly significant effect on the ratio of inlet velocity to tangential flow velocity, coupled with the small (0.028 kg/s) mass flow rate

for ARRM, this indicates that velocities within the vessel are small. Thus ignoring forced convection effects is not unreasonable. Churchill and Chu developed an equation for determining the Nusselt number for vertical plates valid over the entire range of Rayleigh numbers (Ref. 7).

$$\overline{\mathrm{Nu}}_{\mathrm{VP}} = \left\{ 0.825 + \frac{0.387\mathrm{Ra}_L^{1/6}}{\left[1 + \left(0.492/\mathrm{Pr} \right)^{\frac{9}{16}} \right]^{\frac{8}{27}}} \right\}^2 \tag{4}$$

$\mathrm{Nu}_{\mathrm{VP}}$ is the average Nusselt number for a vertical flat plate; Ra is the Rayleigh number, which is the product of the Grashof and Prandtl numbers; and Pr is the Prandtl number of the gas. When loaded on the spacecraft, the COPVs can be treated as vertical cylinders for obtaining the heat transfer coefficients. The general criterion for treating a vertical cylinder as a vertical flat plate in determining the Nusselt number for natural convection is

$$\frac{D}{L} \geq \frac{35}{\mathrm{Gr}_L^{0.25}} \tag{5}$$

where D is the diameter of the tank, L is the overall length of the tank, and Gr is the Grashof number (Ref. 7). D/L for the ARRM Block 1 Baseline is 0.25; the $35/\mathrm{Gr}_L^{0.25}$ ratio throughout the analysis performed was always less than 0.05 for the inside surface and less than 0.06 for the outside surface, so the criterion holds true for each surface of the vessel, and the cylinder can be treated as a vertical flat plate when considering natural convection.

Heat transfer between the outside surface of the tank wall and the ambient environment is governed by Equation (6) (Ref. 4):

$$\dot{Q}_\infty = \left(h_q A_w \right)_\infty \left(T_w - T_\infty \right) \tag{6}$$

The external heat transfer coefficient is determined from either natural or forced convection effects. Thus Equation (4) was also used in determining the Nusselt number for free convection on the vessel exterior surface when no cooling flow is applied.

The cooling method considered is forced flow along the axial direction of the COPV (Fig. 2). The velocity (v_∞) and temperature (T_∞) of the cooling fluid were varied, and the effect of this variance on xenon temperature throughout loading were studied. In this analysis, the cooling fluid used is air. Wiberg and Lior (Ref. 8) determined empirical correlations for forced convection along the axial direction of a cylinder of the form

$$\mathrm{Nu} = C\,\mathrm{Re}^e \tag{7}$$

where Re is Reynolds number based on the diameter of the cylinder, and C and e are empirical constants based on the configuration of the experiment. For laminar flow ($\mathrm{Re} < 5\times10^5$), C is equal to 1.34 and e equals 0.668. For transitional flow occurring around $\mathrm{Re} = 5\times10^5$, $C = 0.155$ and $e = 0.674$ with 6.7 percent turbulent flow; these values were used when $\mathrm{Re} > 5\times10^5$. The valid range of Reynolds numbers for these empirical correlations is $\mathrm{Re} = 8.8\times10^4$ to $\mathrm{Re} = 6.17\times10^5$ (Ref. 8).

Combining Equation (1) with Equation (3), Equation (2) with Equation (6), then simplifying and making some substitutions such as $h_0 = c_p T_0$ results in a pair of differential equations that contain the change in both gas and wall temperature as a function of mass inside the vessel. Equations (8) and (9) are the ordinary differential equations governing the nonadiabatic charging of a pressure vessel (Ref. 4).

$$\dot{m} * m\left(\frac{dT}{dm}\right) + \left[\frac{\left(h_q A_w\right)_i}{C_v}\right]\left(T - T_w\right) + \dot{m}\left(T - \gamma T_{0\text{in}}\right) = 0 \tag{8}$$

$$\dot{m}\left(\frac{dT_w}{dm}\right) + \left[\frac{\left(h_q A_w\right)_i + \left(h_q A_w\right)_\infty}{\left(W_c\right)_w}\right] T_w - \left[\frac{\left(h_q A_w\right)_i}{\left(W_c\right)_w}\right] T - \left[\frac{\left(h_q A_w\right)_\infty}{\left(W_c\right)_w}\right] T - \left[\frac{\left(h_q A_w\right)_\infty}{\left(W_c\right)_w}\right] T_\infty = 0 \tag{9}$$

In Equations (8) and (9), $\dot{m}$ is mass flow rate of the gas, m is the mass of gas inside the tank, T is temperature, γ is the ratio of specific heats of the gas, h_q is a convection coefficient, A is tank wall area, c_v is the specific heat at constant volume of the gas, and W_c is thermal capacitance of the tank wall. Subscript i indicates a condition inside the COPV, subscript 0 indicates a stagnation property, subscript w indicates a property of the tank wall, subscript ∞ indicates an ambient condition outside the tank, and subscript "in" indicates a property of the inlet gas (Ref. 4).

Thermodynamic and transport fluid properties such as c_v and thermal conductivity of xenon were calculated using the National Institute of Standards and Technology (NIST) program REFPROP (Reference Fluid Thermodynamic and Transport Properties Program). The differential equations were solved by substituting $\frac{dT}{dm}$ and $\frac{dT_w}{dm}$ with $\frac{\Delta T}{\Delta m}$ and $\frac{\Delta T_w}{\Delta m}$ and performing a marching analysis by marching time using a time step Δt. Since $\dot{m}$ is constant, Δm is also known throughout the marching analysis, which allows ΔT and ΔT_w to be solved for after each time step. The temperature at time step j is calculated through $T_j = T_{j-1} + \Delta T_{j-1}$, which is a forward marching numerical method. The calculated temperature and density of gas inside the tank were input into REFPROP to determine the pressure of xenon inside the COPV. A uniform gas temperature within the tank is assumed.

Analysis Results

Initially, a mass flow rate of 100 kg/hr was studied; this rate allows the tank fill to be completed in 12.5 hr. Temperature and pressure profiles are presented for three different cooling scenarios:

(1) No active cooling is applied to the COPV. The only means for the COPV to reject heat is natural convection to the ambient air.
(2) Air at ambient temperature (20 °C) is blown over the COPV at 5 m/s to provide forced convection cooling.
(3) Chilled air at 0 °C is blown over the COPV at 5 m/s.

Figure 3 shows an end view of the spacecraft and the "bottle farm" for the interim design analysis cycle 3 (IDAC–3) configuration. An annulus allows for external flow to be applied to cool the COPVs through forced convection methods.

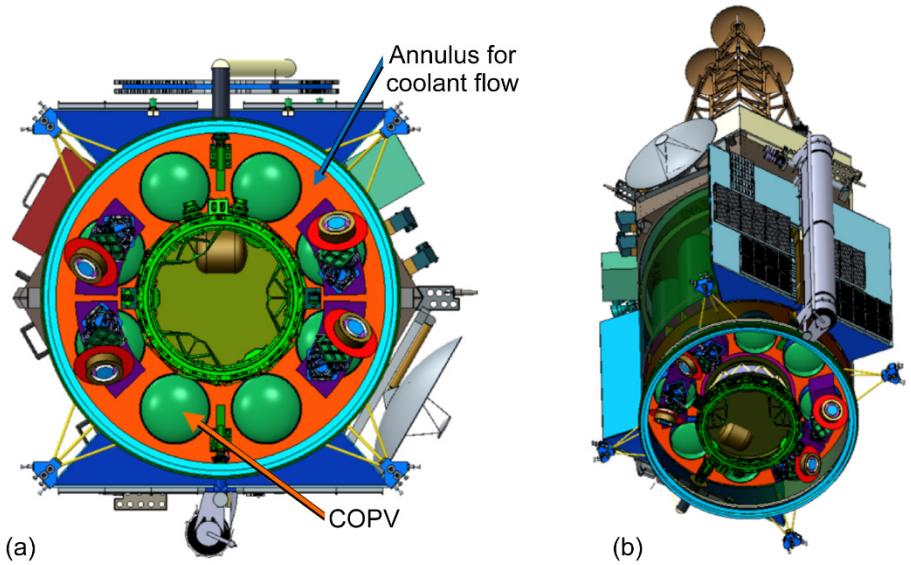

Figure 3.—Post-MCR (Mission Concept Review) interim design analysis cycle 3 (IDAC–3) Block 1 configuration containing eight composite overwrapped pressure vessels (COPVs) with aluminum liners. Cooling air will flow through the annulus area during flight tank loading (Ref. 2).

The first of several cooling scenarios analyzed used no active forced convection cooling. The only outside surface heat transfer to occur was natural convection between the tank wall and surrounding air at a constant 21 °C. The results, plotted in Figure 4, reveal a dramatic temperature spike during the onset of loading. Dicken noted that for the charging of tanks with hydrogen, "the greatest increase in temperatures occurs at the onset of filling and the rate of temperature increase gradually diminishes throughout the fill" (Ref. 9). At the beginning of filling, the inside of the tank contains the lowest amount of gas, and that mass has the lowest thermal capacitance; therefore it is at the onset of filling that the temperature of the gas inside the vessel is most affected by the heat of compression. The same logic can be applied to xenon, and this is in agreement with the predicted temperature increase in Figure 4. The temperature spikes to 50 °C, drops about 5 °C, then steadily rises to a peak temperature of 105 °C at time 550 min; the temperature then drops about 11 °C during the last 350 min of loading. The tank pressure steadily rises throughout loading from 14.7 to 3410 psia. Results from this analysis indicate that some sort of active cooling will be required to keep the xenon temperature below 55 °C during loading, as the tank would have burst during this loading scenario.

Figure 5 displays the xenon temperature and pressure profile after introducing cooling airflow at 5 m/s and 21 °C. The temperature spikes to 54 °C at the beginning of loading. For both the external flow case and the no flow case, the xenon temperature follows the same profile throughout the fill. The temperature spikes at the onset of loading, decreases rapidly, increases to a peak temperature when loading is two-thirds complete, and then decreases for the remainder of loading. At these cooling conditions the peak temperature is 65 °C and peak pressure is 2175 psia.

Next the velocity was held at 5 m/s but the air temperature was decreased to 0 °C. The results are plotted in Figure 6. Note that decreasing the air temperature by 21 °C at this velocity decreased the peak xenon temperature by 10 °C and prevented the maximum temperature from exceeding 55 °C. The xenon is at 42 °C and 1755 psia at the completion of loading. The requirement for the xenon to be at 1750 psia and 40 °C at the completion of loading accommodated the design of the 30-in.-diameter pre-MCR vessel. The gas density at a fully loaded condition is slightly less than the 30-in. tank for the post-MCR 23-in.-diameter tank. When this smaller tank is fully loaded at 40 °C, the pressure will actually be closer to 1700 psia. This "extra volume" allows for some additional margin on the final tank temperature, as the design pressure remains 1750 psia for the post-MCR flight tank.

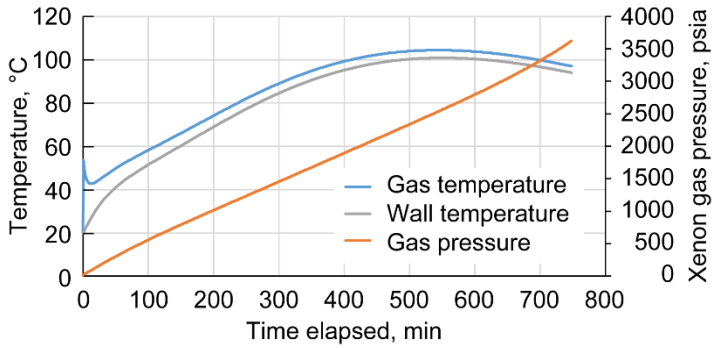

Figure 4.—Xenon gas temperature and pressure throughout loading at fill rate of 100 kg/hr with no forced convection cooling.

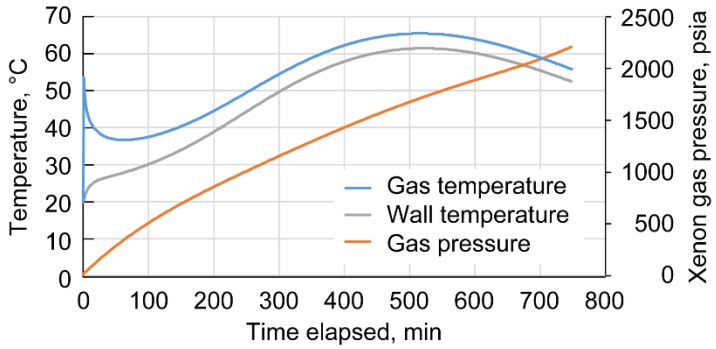

Figure 5.—Xenon temperature and pressure profile for loading post-MCR (Mission Concept Review) tank at 100 kg/hr using air coolant at 5 m/s and 20 °C.

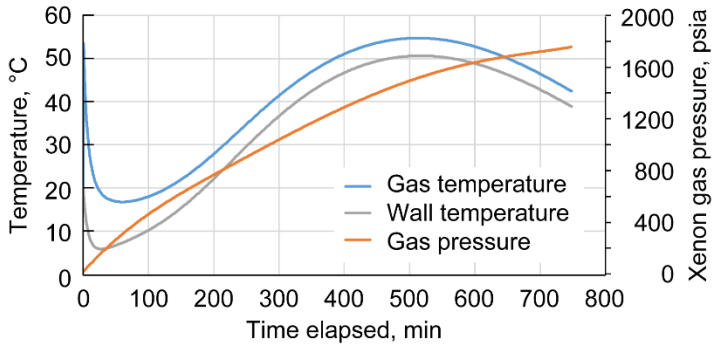

Figure 6.—System temperatures and pressures during loading of post-MCR (Mission Concept Review) tank design using air coolant at 5 m/s and 0 °C.

The effects of coolant velocity and temperature on xenon temperature and pressure were analyzed parametrically. Table II presents a summary of the results. The fill rate used in the Table II simulations was 100 kg/hr. The green highlighted rows indicate that the final pressure and temperature requirements are satisfied for a given coolant condition. From the table it is evident that to meet the final temperature and pressure requirement either the mass flow rate of the coolant must be increased or the coolant temperature must be decreased for a given flow rate.

Each of the coolant conditions listed in Table II has an associated flow rate required to pass the coolant through the annulus shown in Figure 3. Figure 7(a) is a conceptual illustration of the coolant flow path during ground loading of the flight tanks. Figure 7(b) presents a simplified view of Figure 3 and shows the areas used to calculate the open area of the flow path A_{bus}. A_1, A_2, and A_3 are known areas, so the bus area is calculated through $A_{bus} = A_1 - (8A_2 + A_3) = 37.2$ ft^2.

TABLE II.—XENON PEAK PRESSURE AND KEY TEMPERATURES WHILE LOADING AT 100 kg/hr

Coolant velocity, m/s	Coolant temperature, °C	Peak xenon temperature, °C	Final xenon temperature, °C	Peak/final xenon pressure, psia
2	20	79	70	2689
5	20	65	55	2179
8	20	59	49	1972
14[a]	20[a]	49[a]	40[a]	1673[a]
2	10	74	64	2471
5	10	60	49	1957
8[a]	10[a]	53[a]	42[a]	1747[a]
2	0	69	54	2370
5[a]	0[a]	55[a]	43[a]	1755[a]
8	0	49	36	1546

[a]Satisfies final pressure and temperature requirements for given coolant condition.

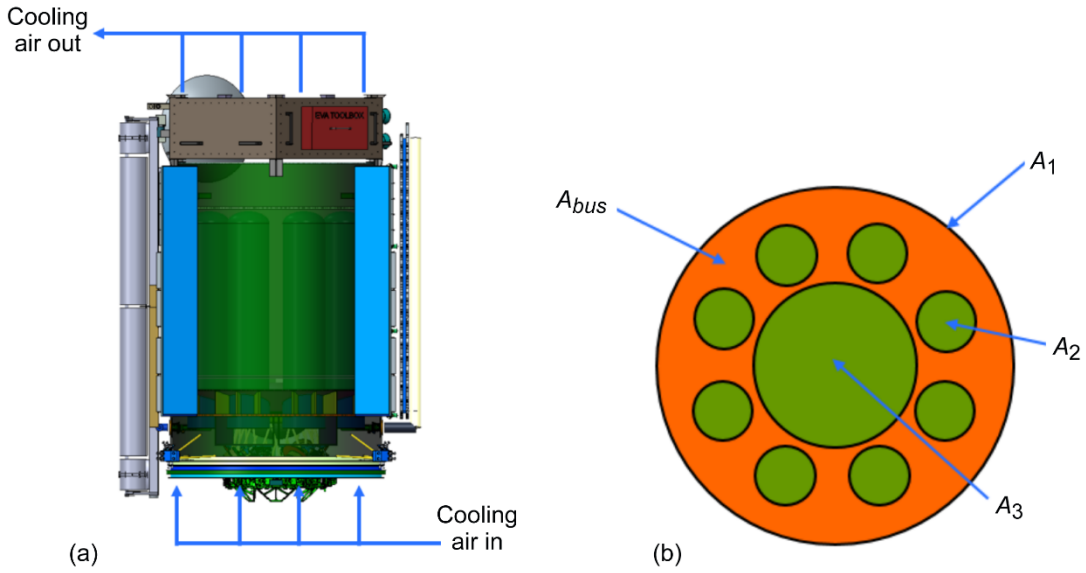

Figure 7.—Post-MCR (Mission Concept Review) interim design analysis cycle 3 (IDAC–3) configuration. (a) Coolant flow path. (b) Spacecraft inner housing cylinder area (A_1), flight composite overwrapped pressure vessel (COPV) area (A_2), support for housing hydrazine tank (A_3), and area in the spacecraft bus through which coolant will flow (A_{bus}) (Ref. 2).

Once the area of the spacecraft bus, A_{bus}, is calculated, the flow rate in actual cubic feet per minute (ACFM) can be obtained by converting the coolant velocity to feet per minute using the conversion factor 1 m/s = 196.8504 ft/min and multiplying the velocity by the bus cross-sectional area.

$$ACFM = A_{bus} v_{\infty} \tag{10}$$

The units for area in Equation (10) must be in square feet, and the velocity must be in feet per minute. Equation (11) converts the actual flow rate to a standard flow rate, which is airflow at standard temperature and pressure (STP), 15 °C and 14.7 psia in this case.

$$SCFM = ACFM \left(\frac{T_{STP} + 273}{T_{\infty} 273} \right) \tag{11}$$

In Equation (11), *SCFM* is flow in standard cubic feet per minute, T_{STP} = 15 °C, and T_{∞} is the temperature of the coolant in degrees Celsius. Table III displays the flow rates in SCFM for the coolant parameters in Table II. The green shading indicates the conditions that result in satisfying the final design temperature and pressure requirements.

Figure 8 shows how flow rates vary with velocity and temperature. Temperature has a minimal effect on flow rate, but for a given velocity the lower temperature requires a slightly higher flow rate due to an increase in air density. The difference in flow rate for various temperatures becomes more pronounced at higher velocities. The flow rates obtained for the three design point solutions will aid in designing the external coolant system.

Equation (6) calculates the heat rejected from the COPV and xenon gas system to the surrounding environment. The heat rejection results for different cooling scenarios are displayed in Figure 9. As expected, reducing the coolant temperature for a given velocity increases the heat rejected as it increases the ΔT in Equation (6). Additionally increasing the coolant velocity for a given temperature increases the heat transfer coefficient and thus increases the heat of compression that is removed from the tank. The three coolant conditions that satisfy the final load requirements from Table III all produce roughly the same curve with a maximum heat rejection requirement of 6.2 kW.

TABLE III.—AIR COOLANT FLOW RATES THROUGH SPACECRAFT ANNULUS

Air velocity, m/s	Cooling airflow, SCFM		
	High air temperature, 20 °C	Medium air temperature, 10 °C	Low air temperature, 0 °C
2.0	14,411	14,921	15,467
4.0	28,823	29,841	30,934
5.0	36,029	37,302	38,668[a]
6.5	46,837	48,492	50,268
8.0	57,646	59,683[a]	61,869
10.0	72,057	74,603	77,336
14.0	100,880[a]	104,445	108,271

[a]Satisfies final design temperature and pressure requirements.

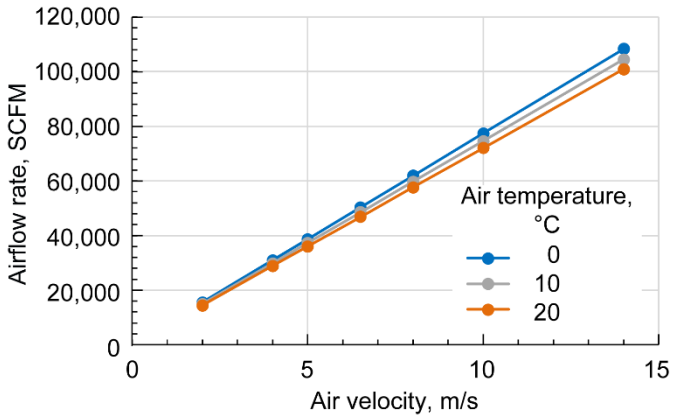

Figure 8.—Air coolant flow rate through spacecraft bus required to achieve various velocities.

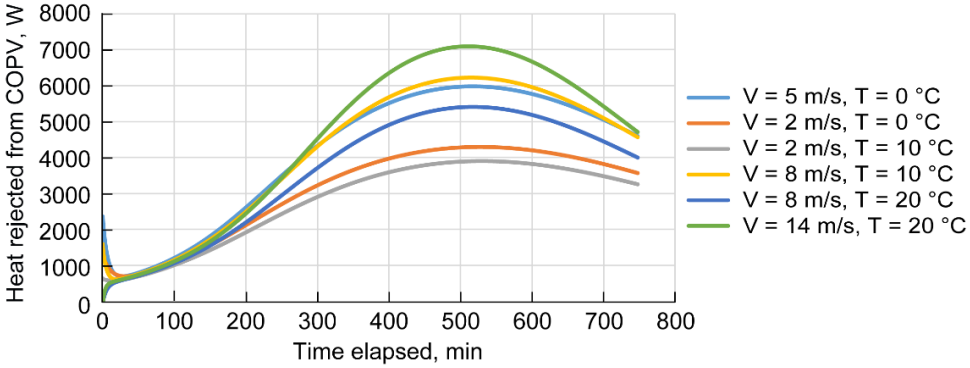

Figure 9.—Heat rejected from composite overwrapped pressure vessel (COPV) for various cooling parameters.

TABLE IV.—COOLANT VELOCITY REQUIRED TO PRODUCE FINAL TEMPERATURE AND PRESSURE OF APPROX. 40 °C AND 1700 psia

Loading time, hr	Inlet xenon mass flow rate, kg/hr	Coolant temperature, °C	Required coolant velocity, m/s	Max. heat rejection, kW
12.50	100.0	10	8	6.2
15.25	82.0	10	6	5.2
20.00	62.5	10	4	4.0

The effect of the mass flow rate of xenon into the COPV on the required coolant velocity and temperature was also studied. Table IV summarizes the results of the three fill rates analyzed. The coolant temperature was held at 10 °C and a velocity was identified that would result in a final xenon temperature of 40±2 °C and 1700±50 psia. Whether or not more than one tank can be loaded simultaneously still needs to be determined; this will dictate what can be considered an acceptable timeline for loading each flight tank with 1250 kg of xenon.

As expected, a lower fill rate reduces the heat of compression generated and therefore reduces the coolant velocity needed to achieve the required final tank temperature and pressure.

Model Validation: Dawn Data Comparison

The Dawn spacecraft, launched in 2007, uses an ion propulsion system with xenon propellant. Although the ARRM spacecraft's eight-tank configuration (shown in Fig. 1) is more complex than Dawn's one-xenon-tank configuration, lessons learned from the Dawn project prompted this analysis of ARRM's xenon loading process. Dawn engineers did not realize active cooling of the xenon tank would be necessary until the flight tank was already imbedded in the spacecraft. They decided to implement a makeshift cooling system in which a cooling tube with vortex coolers was snaked into the cavity just below the xenon tank, where they could then easily control the temperature of the xenon. The lesson learned for ARRM is to include a dedicated ground subsystem that interfaces with the spacecraft and provides cooling of the xenon tanks in the spacecraft design, rather than adding that feature in an ad hoc manner at the last minute (Ref. 1). To prevent temperature excursions, and with cooling provisions in place, the entire 410 kg of xenon, plus the 15 kg already inside the Dawn tank, was loaded in a total elapsed time of 25 hr. The rate at which the xenon could be loaded was directly related to the rate at which the heat from the compression process could be removed from the tank.

Brophy et al. presented graphical mass and pressure versus time data on the ground loading of xenon into Dawn's COPV (Ref. 10). The Dawn xenon loading process is very similar to the proposed ARRM loading requirements, making the reported Dawn data a good source against which to validate the loading model. Table V compares the characteristics of the flight tank used in Dawn with the assumed dimensions of the COPV used in the ARRM analysis. Figure 10 shows the COPV used for the Dawn mission (Ref. 11). The Dawn tank maximum expected operating pressure (MEOP) was eventually derated to a 425 kg load at 1310 psig.

Brophy et al. (Ref. 10) reported data for the xenon mass loaded versus time plot, as shown in Figure 11. The gas temperature had to be back calculated using REFPROP with reference input properties of pressure and density (mass inside the tank divided by the tank volume). The reported mass and time data were then used as inputs to the marching analysis. Additional inputs include the characteristics of the Dawn COPV.

The Dawn COPV used a titanium liner "made from two welded domes that is then over-wrapped with a graphite fiber based composite" (Ref. 12); the ARRM's liner was aluminum. In the absence of additional information about the composite used, it was assumed that the same resin and fiber to be used for ARRM had been used in Dawn and that the liner epoxy-to-fiber ratios were the same for the two missions as well. Thus the same thermal conductivity and specific heat values for the Toray T1000 fiber and epoxy resin used in ARRM were used in the Dawn model.

TABLE V.—CHARACTERISTICS OF COMPOSITE OVERWRAPPED PRESSURE VESSEL (COPV) IN DAWN SPACECRAFT VERSUS ASTEROID REDIRECT ROBOTIC MISSION (ARRM) SPACECRAFT (REF. 11)

Mission	Manufacturer	Diameter, in.	Length, in.	Volume, L	Tank mass, kg	Xenon mass, kg	Maximum expected operating pressure (MEOP), psi
ARRM, post-MCR (Mission Concept Review)	TBD	23.5	120	760	62.5	1250	1750
Dawn	Carleton Technologies Inc.	35.5	26.5	267.9	22.2	450	1750

Figure 10.—Dawn xenon propellant tank (Ref. 11).

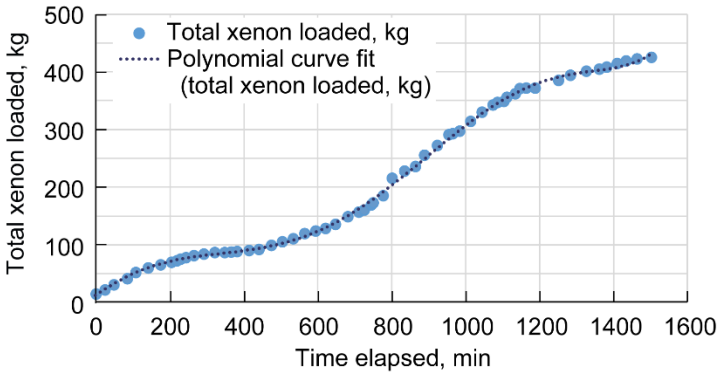

Figure 11.—Xenon mass loaded as function of time, as reported by Brophy et al. (Ref. 10), and polynomial curve fit used to input mass load into model.

Geometrically, the Dawn composite tank has a cylindrical middle section with hemispheres of an oblate spheroid on either side of the cylinder. Table V lists the diameter of the cylinder and the overall height of the vessel. To calculate the heat transfer area of the COPV, an iterative procedure was used that varied the height of the cylinder and the minor radius of the oblate spheroid until the volume of the vessel was within 4 percent of the documented COPV volume. From Figure 10 it is evident that the Dawn flight tank is not a vertical cylinder, so the equations used to determine the Nusselt numbers had to be modified for Dawn. For the inside heat transfer coefficient, the vertical walls of the tank were treated as vertical plates and Equation (4) was used to determine their Nusselt number. The bottom "flatter" surface was treated as the upper surface of a cold plate and Equation (12) was used to determine its Nusselt number. Equations (13) and (14) give the Nusselt number for the lower surface of a cold plate; this number is used for the tank's top surface depending on the Rayleigh number (Ref. 7).

$$\overline{\mathrm{Nu}_L} = 0.27\mathrm{Ra}_L^{1/4} \text{ for } \left(10^5 \le \mathrm{Ra}_L \le 10^{10}\right) \tag{12}$$

$$\overline{\mathrm{Nu}_L} = 0.54\mathrm{Ra}_L^{1/4} \text{ for } \left(10^4 \le \mathrm{Ra}_L \le 10^{7}\right) \tag{13}$$

$$\overline{\mathrm{Nu}_L} = 0.15\mathrm{Ra}_L^{1/3} \text{ for } \left(10^7 \le \mathrm{Ra}_L \le 10^{11}\right) \tag{14}$$

The forced convection coefficient for the exterior surfaces treats the COPV as a sphere and uses Equations (15) and (16) depending on the Reynolds number of the flow (Ref. 13).

$$\mathrm{Nu} = 2 + \left(0.25\mathrm{Re} + 3\times10^{-4}\,\mathrm{Re}^{1.6}\right)^{1/2} \quad \text{for } 100 < \mathrm{Re} < 3\times10^{5} \tag{15}$$

$$\mathrm{Nu} = 430 + 5\times10^{-4}\,\mathrm{Re} + 2.5\times10^{-10}\,\mathrm{Re}^{2} - 3.1\times10^{-17}\,\mathrm{Re}^{3} \quad \text{for } 3\times10^{5} < \mathrm{Re} < 5\times10^{6} \tag{16}$$

Since the frequency of Dawn data points plotted in Brophy was only 24 min, a curve fit for the xenon mass loaded as a function of time was generated so that the time step could be adjusted to produce reasonable results. The mass flow rate as a function of time was determined by taking the derivative of the mass versus time curve. The curve fit is displayed in Figure 11. The Dawn inlet temperature was controlled such that the ambient dew point was avoided; since the temperature was not stated explicitly, the inlet temperature was assumed to be a constant 20 °C during loading, as this satisfies the dew point condition (Ref. 14). The mass loaded and time data were used as inputs to the model in addition to the thermal and geometric properties of the flight tank. The external coolant air velocity and the temperature from the vortex coolers were also not explicitly stated, so these values were varied within reason such that the model better predicted the reported pressure and temperature distributions throughout loading.

Figure 12 compares the reported pressure data for the Dawn flight tank xenon loading with the heat transfer model predictions for two different coolant velocities at 10 °C. Over the first 700 min, the model trend correlates almost perfectly with the reported data trend. Starting at 700 min, the models begin to increasingly overpredict the COPV pressure, with a maximum overprediction of 400 psi at 1000 min into loading. From 1200 to 1400 min, the model begins to underpredict the tank pressure when the tank pressure starts decreasing at 1100 min. At 1100 min, Dawn engineers stopped filling the tank and allowed it to self-heat in order to measure the associated pressure rise as a proof test. The tank cooling was then reestablished, and filling resumed around 1200 min.

The temperature comparison of the heat transfer model prediction with the reported data is displayed in Figure 13. A significant temperature spike occurs at the onset of loading; the xenon temperature increases rapidly from 17 °C to over 40 °C. In this instance the model actually underpredicts the magnitude of the temperature spike. This is likely because cooling hardware was not yet in place during the initial Dawn loading process; only later did it become evident that filling the tank in a timely manner would require cooling provisions. In the model, cooling is present during the entire loading cycle, which decreases the magnitude of the initial spike in temperature. The 20 m/s and 10 °C coolant model varies between overpredicting and underpredicting the temperature throughout loading by about 15 °C. However, the shape of the curves generated by the model follow the temperature trends of the derived xenon temperatures from the reported mass and pressure data. The final temperature for this model matches almost exactly the actual final temperature reported at the end of loading. The 20 m/s and 20 °C coolant model matches temperatures very well through the beginning and end of loading, but between 600 and 1000 min, the model significantly overpredicts the temperature.

While the modeling approach could not exactly reproduce the reported Dawn data, the comparisons are accurate enough (within times 0 to 600 min and 1200 to 1500 min) to consider the modeling approach validated at an accuracy level sufficient for a first look at analyzing the gas temperature and pressure profiles throughout loading. The major source of error in the temperature profile is that constant external coolant parameters were used throughout the entire model, whereas Dawn engineers implemented cooling after loading began and varied their coolant parameters to maintain the xenon temperature in a desired range. Thus between 600 and 1000 min the model coolant parameters would need to be increased in order to better match the reported data; but the constant coolant velocity and temperature limitation in the model prevent this, and an overprediction in temperature is observed. The model heat transfer approach was also validated against data obtained from the loading of a COPV with hydrogen.

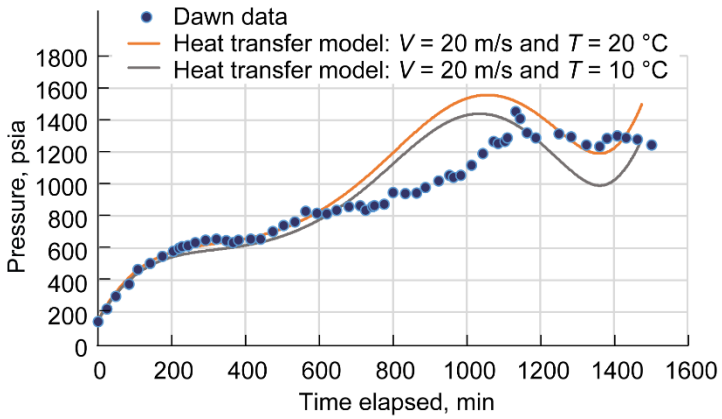

Figure 12.—Dawn pressure data versus model-predicted pressure.

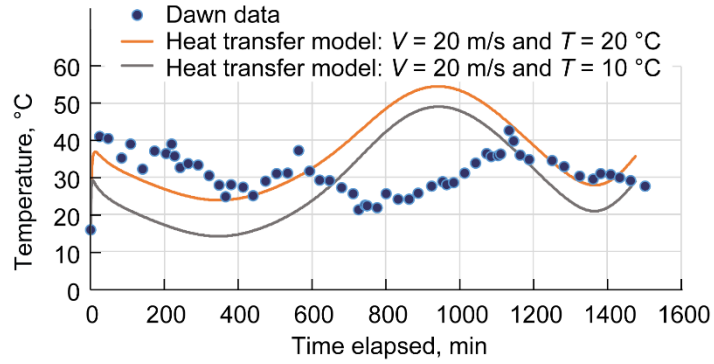

Figure 13.—Dawn temperature data versus model-predicted temperature.

Model Validation: Hydrogen Loading Data Comparison

The following plots compare pressure and temperature data tabulated in "A Thermodynamic Model for a High-Pressure Hydrogen Gas Filling System Comprised of Carbon-Fibre Reinforced Composite Pressure Vessels" by Woodfield and Monde (Ref. 15) with pressures and temperatures predicted by inputting time and mass loaded into the Excel model. A difference between these validation cases and the ARRM model previously described is that the ARRM model assumed a constant mass flow rate throughout loading, whereas each of the validation models (Dawn and rapid H_2 fill) had a variable mass flow rate. In these instances, a curve fit was applied to the reported mass flow data as a function of time so that time, mass flow rate, and mass inside the COPV could be used as inputs to the model. The mass loaded versus time plot and the second-order polynomial curve fit used in this validation case are displayed in Figure 14.

Additional inputs to the model include the material, thermal, and geometric properties of the COPV. The tank surface area used for heat transfer calculations was determined using the same approach as the Dawn validation case. Like the ARRM COPV, the COPV in this model uses an aluminum liner that is 0.17 in. (4.25 mm) thick; the carbon fiber reinforced plastic is 0.67 in. (17 mm) thick. Table VI displays the properties of the carbon fiber material of the COPV in the rapid hydrogen filling model (Ref. 15).

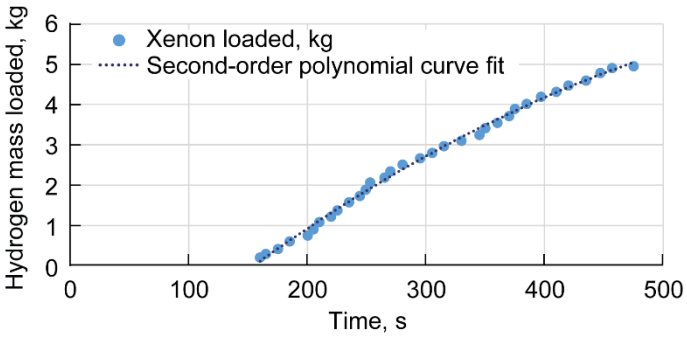

Figure 14.—Hydrogen mass loaded data as function of time reported by Woodfield and Monde (Ref. 15) and curve fit used to input mass load into model.

TABLE VI.—PROPERTIES OF COMPOSITE OVERWRAPPED PRESSURE VESSEL (COPV) USED IN RAPID HYDROGEN FILLING VALIDATION MODEL

Thermal diffusivity, m^2/s	4.5×10^{-7}
Thermal conductivity, W/m-K	0.55
Density, kg/m^3	1,530
Specific heat, J/kg-K	799
Overall COPV thermal capacitance (including aluminum liner), J/K	68,008

Equation (17) is an empirical correlation determined by Woodfield and Monde (Ref. 15) for the Nusselt number they used in determining the model's inside surface convection coefficient in the model they developed in their 2010 study. The validation model was run twice. One case uses Equation (4) for the inside surface Nusselt number; the other uses Equation (17).

$$\mathrm{Nu}_D = 0.56\,\mathrm{Re}_d^{0.67} + 0.104\,\mathrm{Ra}_D^{0.352} \tag{17}$$

In Equation (17), Re_d is the Reynolds number based on the inlet pipe diameter and inlet flow velocity; Ra_D is the Rayleigh number based on the COPV diameter (Ref. 15). Figure 15 compares the model-predicted pressures with the reported pressure data.

For hydrogen pressure, the difference between using Equation (4) or Equation (17) for the inside surface Nusselt number appears negligible. The model does an excellent job of predicting the experimental pressure throughout the entire fill. The overprediction error near the end of loading is likely attributable to using a curve fit to predict the hydrogen mass loaded as a function of time. This curve fit is necessary so that a sufficiently small time step can be chosen; for this model, the time step used was 0.5 sec.

Figure 16 shows the model-predicted temperatures versus the reported hydrogen temperature throughout the rapid loading process. The deviation in temperature between the two Nusselt number equation cases is much larger than the deviation in pressure. Equation (16) more accurately predicts the temperature than does Equation (4), following the data trend almost exactly with a maximum deviation of about 5 °C. This makes intuitive sense, as Equation (17) is an empirical correlation developed specifically for this application and Equation (4) is a general flat plate equation. The model using Equation (4) predicts a temperature spike from 8 to 62 °C, whereas the data indicates that the temperature only spikes to about 50 °C. After the initial spike, the model prediction follows the reported data trend quite closely starting at 250 sec. Figures 12, 13, 15, and 16 indicate that the heat transfer modeling approach taken can predict the actual temperature and pressure profiles of a gas during tank pressurization, including the temperature spike at the onset of loading.

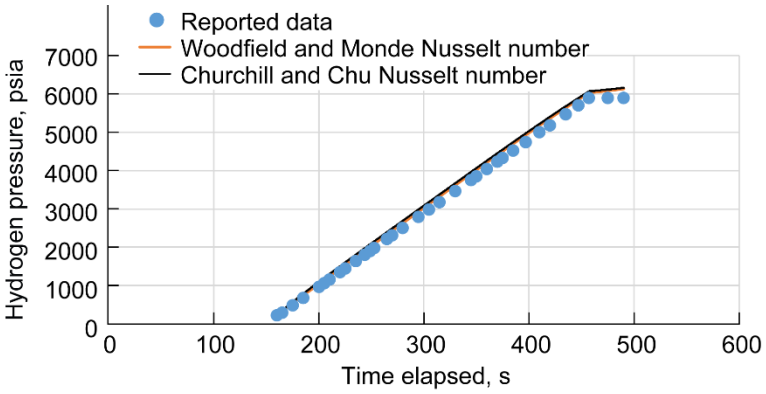

Figure 15.—Model-predicted hydrogen pressure versus Woodfield and Monde's measured hydrogen pressure data (Ref. 15).

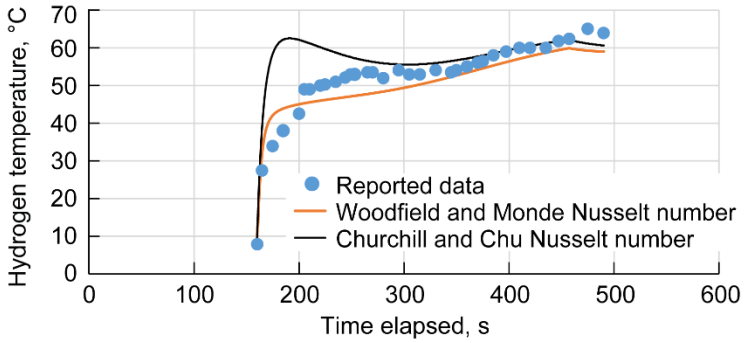

Figure 16.—Model-predicted hydrogen temperature versus Woodfield and Monde's measured hydrogen pressure data (Ref. 15).

Summary of Results

A Microsoft Excel model using the governing thermodynamic and heat transfer equations was created to simulate the loading of 1250 kg of xenon into a flight composite overwrapped pressure vessel (COPV). The model calculated an internal convection coefficient between the gas and tank wall as well as an external heat transfer coefficient to account for the effects of forced and free convection. The effects of varying external coolant velocity and temperature were analyzed parametrically. Using external coolant significantly reduced the xenon temperature and pressure throughout loading. Several coolant velocities and temperatures were identified that would keep the xenon temperature below 55 °C at all times and result in a final temperature of target conditions close to 40 °C and 1750 psia. The coolant mass flow rate and temperature requirements from the analysis will aid in the design of the COPV active cooling subsystem at the launch facility for the Asteroid Redirect Robotic Mission (ARRM) spacecraft.

This heat transfer modeling approach was validated against flight and test datasets: (1) data from the Dawn mission's xenon flight tank loading experience and (2) data from a study of the rapid loading of hydrogen into a COPV (Ref. 15). The successful validation effort inspires confidence that the results of this trade study are accurate enough to begin designing the ground support equipment to be used for loading xenon into the ARRM spacecraft.

Appendix—Nomenclature

Acronyms

ACFM	actual cubic feet per minute
ARRM	Asteroid Redirect Robotic Mission
CFD	computational fluid dynamics
COPV	composite overwrapped pressure vessel
IDAC	interim design analysis cycle
MCR	Mission Concept Review
MEOP	maximum expected operating pressure
NIST	National Institute of Standards and Technology
REFPROP	Reference Fluid Thermodynamic and Transport Properties Program
SCFM	standard cubic feet per minute
SEP	solar electric propulsion
STP	standard temperature and pressure

Symbols

A	area
A_{bus}	area through which coolant will flow
A_w	wall area of pressure vessel
A_1	cross section of spacecraft bus for coolant flow
A_2	area designation for xenon tanks
A_3	area in cross section of spacecraft for hydrazine tank
$ACFM$	flow rate in actual cubic feet per minute
C	empirical constant used in Equation (7)
c_p	specific heat at constant pressure
c_v	specific heat at constant volume
D	COPV cylinder diameter
d	diameter of inlet pipe to COPV
e	empirical constant used in Equation (7)
g	gravitational constant, 9.81 m/s^2
Gr	Grashof number, $\mathrm{Gr} = \dfrac{g\beta\left(T_s - T_f\right)L^3}{\left(\mu/\rho\right)^2}$
h	specific static enthalpy
h_0	specific stagnation enthalpy
$h_{0\mathrm{in}}$	stagnation enthalpy of gas entering tank
h_q	convection coefficient
k	thermal conductivity
L	COPV length
m	mass
$\dot{m}$	mass flow rate

Nu	Nusselt number, $\mathrm{Nu} = \frac{h_q * L}{k}$
Nu_{VP}	Nusselt number for vertical flat plate
P	pressure
Pr	Prandtl number, $\mathrm{Pr} = \frac{\mu c_p}{k}$
$\dot{Q}$	heat transfer rate
$\dot{Q}_i$	heat transfer rate between gas and tank inside wall surface
$\dot{Q}_\infty$	heat transfer rate between tank outside wall surface and ambient environment
Ra	Rayleigh number, $\mathrm{Ra} = \mathrm{Gr}\,\mathrm{Pr}$
Re	Reynolds number, $\mathrm{Re} = \frac{\rho v L}{\mu}$
$SCFM$	flow rate in standard cubic feet per minute
T	temperature
T_f	fluid temperature
T_s	surface temperature
T_{STP}	standard temperature (15 °C)
T_w	uniform COPV wall temperature
T_0	stagnation temperature
T_∞	ambient temperature
t	time
u	specific internal energy
v	velocity
v_∞	velocity of coolant gas outside tank
W_c	thermal capacitance of COPV wall
Z	compressibility factor
β	volume expansion coefficient
γ	ratio of gas specific heats, $\frac{c_p}{c_v}$
μ	dynamic viscosity
ρ	density

References

1. Brophy, John: Dawn Lessons Learned—IPS (Final) for Goebel. Lessons Learned 40 and 41. NASA Internal Excel File. Available from the Office of the Chief Engineer.
2. Cressman, Thomas O.: Xenon Loading. NASA Glenn ARRM Structures team presentation, unpublished, 2014.
3. Tomsik, Thomas; and Gilligan, Ryan: ARRM SEP Post-MCR Status Report. NASA Internal Document, 2014. Available from the NASA STI Program.
4. Kunkle, John S.; Wilson, Samuel D.; and Cota, Richard A., eds.: Compressed Gas Handbook. NASA SP–3045, 1969. http://ntrs.nasa.gov
5. Lyons III, John Thomas: Heat Transfer Considerations in a Pressure Vessel Being Charged. M.S. Thesis, United States Naval Postgraduate School, 1969, p. 59. http://www.dtic.mil/dtic/tr/fulltext/u2/706713.pdf Accessed March 8, 2017.
6. Ranong, Chakkrit Na, et al.: Approach for the Determination of Heat Transfer Coefficients for Filling Processes of Pressure Vessels With Compressed Gaseous Media. Heat Transfer Eng., vol. 32, no. 2, 2011, pp. 127–132. http://www.tandfonline.com/doi/pdf/10.1080/01457631003769187 Accessed March 8, 2017.
7. Bergman, Theodore L., et al.: Fundamentals of Heat and Mass Transfer. John Wiley & Sons, Inc., Hoboken, NJ, 2013.
8. Wiberg, Roland; and Lior, Noam: Heat Transfer From a Cylinder in Axial Turbulent Flows. Int. J. Heat Mass Transfer, vol. 48, 2005, pp. 1505–1517. http://www.seas.upenn.edu/~lior/documents/HeattransferfromacylinderinaxialIJHMT.pdf Accessed March 8, 2017.
9. Dicken, Christopher John Bruce: Temperature Distribution Within a Compressed Gas Cylinder During Filling. A Thesis Submitted in Partial Fulfillment of the Requirements for the Degree of Master of Applied Science, University of British Columbia, 2006, p. 75.
10. Brophy, John R., et al.: The Dawn Ion Propulsion System—Getting to Launch. IEPC–2007–083, 2007.
11. Hofer, Richard R., et al.: Evaluation of a 4.5 kW Commercial Hall Thruster System for NASA Science Missions. AIAA–2006–4469, 2006.
12. Jet Propulsion Laboratory: COPV Propellant Tank Failure on the Dawn Spacecraft. Lesson Number 1777, 2007. http://llis.nasa.gov/lesson/1777 Accessed March 8, 2017.
13. Holman, J.P.: Heat Transfer. 9th Ed., McGraw-Hill, New York, NY, 2002.
14. Mizukami, M.; Nakazono, B.; and Klatte, M.F.: Dawn Spacecraft Ion Propulsion System Xenon Loading Operation. Jet Propulsion Laboratory, unpublished report, 2008.
15. Woodfield, P.L.; and Monde, M.: A Thermodynamic Model for a High-Pressure Hydrogen Gas Filling System Comprised of Carbon-Fibre Reinforced Composite Pressure Vessels. Presented at the 17th Australasian Fluid Mechanics Conference, Aukland, New Zealand, 2010.